JB THE JOURNAL OF BIOCHEMISTRY

2′-*O*,4′-*C*-ethylene bridged nucleic acid modification enhances pyrimidine motif triplex-forming ability under physiological condition

Hidetaka Torigoe*, Norihiro Sato and Nobuyuki Nagasawa

Department of Applied Chemistry, Faculty of Science, Tokyo University of Science, 1-3 Kagurazaka, Shinjuku-ku, Tokyo 162-8601, Japan

*Hidetaka Torigoe, Department of Applied Chemistry, Faculty of Science, Tokyo University of Science, 1-3 Kagurazaka, Shinjuku-ku, Tokyo 162-8601, Japan. Tel: +81-3-5228-8259, Fax: +81-3-5261-4631, email: htorigoe@rs.kagu.tus.ac.jp

Since pyrimidine motif triplex DNA is unstable at physiological neutral pH, triplex stabilization at physiological neutral pH is important for improvement of its potential to be applied to various methods *in vivo*, such as repression of gene expression, mapping of genomic DNA and gene-targeted mutagenesis. For this purpose, we studied the thermodynamic and kinetic effects of a chemical modification, 2′-*O*,4′-*C*-ethylene bridged nucleic acid (ENA) modification of triplex-forming oligonucleotide (TFO), on pyrimidine motif triplex formation at physiological neutral pH. Thermodynamic investigations indicated that the modification achieved more than 10-fold increase in the binding constant of the triplex formation. The increased number of the modification in TFO enhanced the increased magnitude of the binding constant. On the basis of the obtained thermodynamic parameters, we suggested that the remarkably increased binding constant by the modification may result from the increased stiffness of TFO in the unbound state. Kinetic studies showed that the considerably decreased dissociation rate constant resulted in the observed increased binding constant by the modification. We conclude that ENA modification of TFO could be a useful chemical modification to promote the triplex formation under physiological neutral condition, and may advance various triplex formation-based methods *in vivo*.

Triplex nucleic acid has recently attracted remarkable interest owing to its possible biological functions *in vivo* and its various potential applications, such as artificial repression of gene expression by antigene strategy, mapping of genomic DNA and gene-targeted mutagenesis (*1–5*). A triplex nucleic acid is usually formed when a single-stranded homopyrimidine or homopurine triplex-forming oligonucleotide (TFO) binds with the major groove of a homopurine—homopyrimidine stretch in duplex DNA with high sequence specificity (*3, 4*). In the pyrimidine motif triplex, a homopyrimidine TFO binds parallel to the homopurine strand of the target duplex by Hoogsteen hydrogen bonding (*3, 4*). The formed typical base triplets for the pyrimidine motif triplex are T•A:T and C⁺•G:C (*3, 4*). In the meantime, in the purine motif triplex, a homopurine TFO binds anti-parallel to the homopurine strand of the target duplex by reverse Hoogsteen hydrogen bonding (*3, 4*). The formed typical base triplets for the purine motif triplex are A•A:T (or T•A:T) and G•G:C (*3, 4*).

Since the cytosine bases in a homopyrimidine TFO should be protonated upon binding with the guanine bases of the G:C target duplex, a condition with acidic pH is necessary for the formation of the pyrimidine motif triplex. Thus, the pyrimidine motif triplex is unstable at physiological neutral pH (*6–8*). In the meantime, the formation of the purine motif triplex is possible at physiological neutral pH due to its pH independence. However, physiological concentrations of certain monovalent cations, especially K⁺ ions, severely inhibit purine motif triplex formation (*9, 10*). The undefined interaction between K⁺ and the guanine-rich homopurine TFO may be involved in this inhibitory effect (*9, 10*). Thus, the stabilization of the pyrimidine motif triplex at physiological neutral pH is important for improvement of its potential to be applied to various triplex formation-based methods. Substitution of 5-methylcytosine (*7, 11–13*) or other chemically modified base derivatives (*14–18*) for the cytosine bases in a homopyrimidine TFO and attachment of different DNA intercalators to the ends of TFO (*19, 20*) have been applied to overcome the necessity of an acidic pH for the pyrimidine motif triplex formation and to increase the stability of the pyrimidine motif triplex at physiological neutral pH.

We formerly investigated the thermodynamic parameters of the pyrimidine motif triplex formation by isothermal titration calorimetry (ITC) (*21*). We found that one of the major factors of entropy change monitored upon triplex formation may come from a negative conformational entropy change resulting from the conformational restriction of the TFO upon the

association with the target duplex to form triplex (*21*). The negative conformational entropy change may be undesirable for the triplex formation. We hypothesized that the increase in stiffness of TFO in the unbound state to reduce the conformational entropy loss upon the triplex formation may promote the triplex formation. Therefore, to enhance the triplex-forming ability by increasing stiffness of TFO in the unbound state, a novel type of chemical modifications of nucleic acids, 2'-*O*,4'-*C*-ethylene bridged nucleic acid (ENA) (Fig. 1A), in which 2'-*O* and 4'-*C* of the sugar group were connected with the ethylene chain (*22*), was synthesized and developed. The thermodynamic stability of the triplex involving ENA-modified TFO at physiological neutral pH was remarkably higher than that involving the corresponding phosphodiester TFO, which was obtained from the UV profile of the melting process of the triplex (*23*). However, the formation process of the triplex involving ENA-modified TFO at physiological neutral pH has not yet been analysed. To examine the possibility of the application of ENA-modified TFO to various triplex formation-based methods *in vivo*, the formation process of the triplex involving ENA-modified TFO at physiological neutral pH should be investigated in more detail than the melting process of the same triplex. Furthermore, the mechanism of the ENA modification-mediated triplex stabilization at physiological neutral pH remains to be elucidated. To this end, we have investigated the thermodynamic and kinetic effects of the ENA modification of TFO on pyrimidine motif triplex formation with another base sequence at physiological neutral pH. The pyrimidine motif triplex formation between a 23 bp homopurine–homopyrimidine target duplex (Pur23A•Pyr23T) (Fig. 1B) and its specific

15-mer unmodified homopyrimidine TFO (Pyr15T) (Fig. 1B) or each of ENA-modified homopyrimidine TFOs (ENA7-1, ENA7-2, ENA5-1 and ENA5-2) (Fig. 1B) have been studied by electrophoretic mobility shift assay (EMSA) (*24–28*), UV melting, ITC (*21*, *25*, *26*, *28–32*) and BIACORE interaction analysis system (*25–28*, *32–34*). We found that the ENA modification of TFO achieved >10-fold increase in the binding constant of the pyrimidine motif triplex formation at physiological neutral pH. The increased number of the ENA modification in TFO enhanced the increased magnitude of the binding constant. Kinetic studies have revealed that the considerably decreased dissociation rate constant resulted in the observed increased binding constant by the ENA modification of TFO. The ENA modification to enhance the pyrimidine motif triplex-forming ability at physiological neutral pH would advance various triplex formation-based methods *in vivo*. The mechanism of the ENA modification to enhance the pyrimidine motif triplex-forming ability will be discussed.

Materials and Methods

Preparation of oligonucleotides

We synthesized 23-mer complementary oligonucleotides for the target duplex, Pur23A and Pyr23T (Fig. 1B), a 15-mer unmodified homopyrimidine TFO specific to the target duplex, Pyr15T (Fig. 1B) and a 15-mer non-specific homopyrimidine oligonucleotide, Pyr15NON (Fig. 1B), on an ABI DNA synthesizer by the solid-phase cyanoethyl phosphoramidite method; we then purified them by reverse-phase HPLC on a Wakosil DNA column. We also synthesized and purified the 15-mer ENA-modified homopyrimidine TFOs specific to the target duplex, ENA7-1, ENA7-2, ENA5-1 and ENA5-2 (Fig. 1B), as described previously (*22*). Furthermore, we prepared 5'-biotinylated Pyr23T (Bt-Pyr23T) using biotin phosphoramidite. We determined the concentration of all oligonucleotides by UV absorbance. We annealed complementary strands, Pur23A and Pyr23T, by heating up to 90°C and then slowly cooling to room temperature. We applied the annealed sample on a hydroxyapatite column (BIORAD Inc.) to eliminate excess single strands. We determined the concentration of the duplex DNA (Pur23A•Pyr23T) by UV absorbance, considering that an absorbance of 1 at 260 nm corresponds to a concentration of 50 μg/ml of DNA, with a M_r of 15,180.

EMSA

We performed EMSA experiments by 15% native polyacrylamide gel electrophoresis, as described previously (*25–28*). In 9 μl of the reaction solution, we mixed ^{32}P-labeled Pur23A•Pyr23T duplex (~1 nM) with the specific TFO (Pyr15T, ENA7-1, ENA7-2, ENA5-1 or ENA5-2) at various concentrations and the non-specific oligonucleotide (Pyr15NON) in the reaction buffer [50 mM tris–acetate (pH 7.0), 100 mM NaCl and 10 mM MgCl₂]. We added Pyr15NON not only to achieve the same concentration (1 μM) of TFO in each lane but also to avoid adhesion of the oligonucleotides (duplex and TFO) to plastic surfaces during incubation and loss of the oligonucleotides during processing. After incubation for 6 h at 37°C, 2 μl of 50% glycerol solution containing bromophenol blue was added with keeping the pH and salt concentration of the reaction solutions. We then directly applied samples onto a 15% native polyacrylamide gel prepared in electrophoresis buffer [50 mM tris–acetate (pH 7.0) and 10 mM MgCl₂], and electrophoresis was carried out at 8 V/cm for 16 h at 4°C.

UV melting

We carried out UV melting experiments on a DU-640 spectrophotometer (Beckman Inc.) containing a Peltier-type cell holder. The length of cell path was 1 cm. We collected UV melting curves in buffer A (10 mM sodium cacodylate–cacodylic acid at pH 6.8 containing 200 mM NaCl and 20 mM MgCl₂) at a scan speed of
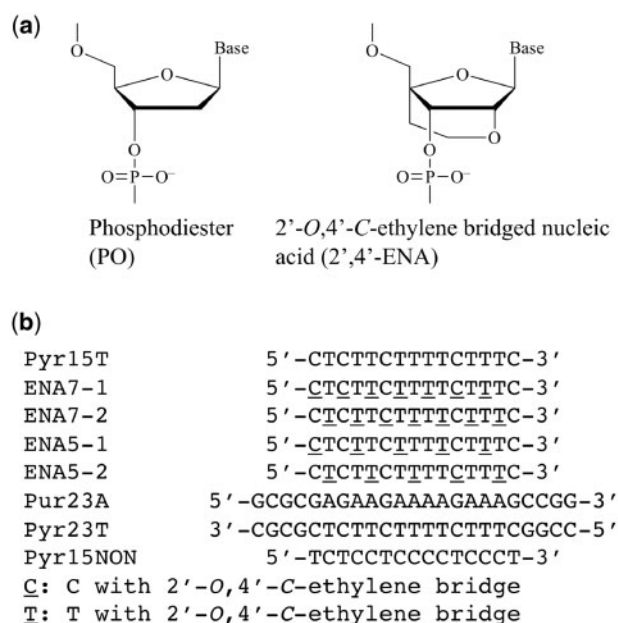

Fig. 1 **Chemical modification of nucleic acids (A) Structural formulas for phosphodiester (PO) and 2'-*O*,4'-*C*-ethylene bridged nucleic acid (ENA)-modified backbones**. (B) Oligonucleotide sequences of the target duplex (Pur23A•Pyr23T), the specific TFOs (Pyr15T, ENA7-1, ENA7-2, ENA5-1 and ENA5-2) and the non-specific oligonucleotide (Pyr15NON).

(a)

Phosphodiester (PO)

2'-*O*,4'-*C*-ethylene bridged nucleic acid (2',4'-ENA)

(b)

```
Pyr15T      5'-CTCTTCTTTTCTTTC-3'
ENA7-1      5'-CTCTTCTTTTCTTTC-3'
ENA7-2      5'-CTCTTCTTTTCTTTC-3'
ENA5-1      5'-CTCTTCTTTTCTTTC-3'
ENA5-2      5'-CTCTTCTTTTCTTTC-3'
Pur23A    5'-GCGCGAGAAGAAAAGAAAGCCGG-3'
Pyr23T    3'-CGCGCTCTTCTTTTCTTTCGGCC-5'
Pyr15NON     5'-TCTCCTCCCCTCCCT-3'
C: C with 2'-O,4'-C-ethylene bridge
T: T with 2'-O,4'-C-ethylene bridge
```

0.5°C/min with monitoring at 260 nm. We obtained the first derivative from the UV melting curve. We designated the peak temperature in the first derivative as the melting temperature T_m. The concentration of triplex nucleic acid was 1 μM.

Circular dichroism spectroscopy

We recorded circular dichroism (CD) spectra at 20°C in buffer A on a JASCO J-720 spectropolarimeter equipped with a microcomputer. The length of cell path was 1 cm. The concentration of triplex nucleic acid was 1 μM.

ITC

We carried out isothermal titration experiments on a VP ITC system (Microcal Inc., USA), as described previously (25, 26, 28). We prepared the TFO and Pur23A•Pyr23T duplex solutions by dialyzing extensively against buffer A or buffer B (10 mM sodium cacodylate–cacodylic acid at pH 5.8 containing 200 mM NaCl and 20 mM MgCl₂). The duplex solution in buffer A or buffer B was injected 25 times in 5 μl aliquots at 10 min intervals into the TFO solution with keeping the reaction conditions. The duplex solution was also injected in the same manner into the experimental buffer without TFO to measure the heat of dilution of the duplex. We subtracted the heat of dilution from the heat of each injection into the TFO solution. We divided each adjusted heat value by the number of moles of the injected duplex and analysed the data with Microcal Origin software provided by the manufacturer.

BIACORE interaction analysis system

We performed kinetic experiments on a BIACORE J instrument (GE Healthcare, USA), where a real-time biomolecular interaction was monitored with a laser biosensor (25–28). The layer of a SA sensor tip containing immobilized streptavidin was equilibrated with buffer A at a flow speed of 30 μl/min. We injected 40 μl of 50 mM NaOH and 1 M NaCl three times at a flow speed of 30 μl/min to decrease electrostatic repulsion from the surface. After equilibrating with buffer A, we added 160 μl of 0.2 μM Bt-Pyr23T•Pur23A duplex solution at a flow speed of 30 μl/min to bind with the streptavidin on the surface. After enough washing and equilibrating the Bt-Pyr23T•Pur23A-immobilized surface with buffer A, we injected 70 μl of the TFO solution in buffer A over the immobilized Bt-Pyr23T•Pur23A duplex at a flow speed of 30 μl/min, and then the triplex formation was observed for 2 min. This was followed by washing the sensor tip with buffer A, and the dissociation of the preformed triplex was observed for an additional 2 min. Finally, 40 μl of 100 mM tris–HCl (pH 8.0) for Pyr15T, 40 μl of 10 mM NaOH (pH 12) for ENA7-1 and ENA7-2 or 40 μl of 3.2 mM NaOH (pH 11.5) for ENA5-1 and ENA5-2 was added at a flow speed of 30 μl/min to completely dissociate the TFO from the Bt-Pyr23T•Pur23A duplex. During the complete dissociation, a part of the Bt-Pyr23T•Pur23A duplex may be unfolded. We regenerated the Bt-Pyr23T•Pur23A duplex by adding 0.2 μM Pur23A. We analysed the obtained profiles with the BIA evaluation software provided by the manufacturer to estimate the kinetic parameters.

Results

EMSA of pyrimidine motif triplex formation at physiological neutral pH

We investigated the pyrimidine motif triplex formation between the target duplex (Pur23A•Pyr23T) (Fig. 1B) and its specific unmodified (Pyr15T) (Fig. 1B) or ENA modified (ENA7-1, ENA7-2, ENA5-1 or ENA5-2) (Fig. 1B) TFO at pH 7.0 by EMSA (Fig. 2). Total concentration of oligonucleotides [specific TFO (Pyr15T, ENA7-1, ENA7-2, ENA5-1 or ENA5-2) (Fig. 1B)] + [non-specific oligonucleotide (Pyr15NON) (Fig. 1B)] for each of triplex formation was held constant at 1 μM to avoid loss of the oligonucleotides during processing and to examine sequence specificity of triplex formation. Although no shift in the electrophoretic mobility of the target duplex was

observed for 1 μM Pyr15NON alone (see lane 1 for Pyr15T), reduction of the duplex mobility due to triplex formation was achieved for Pyr15T, ENA7-1, ENA7-2, ENA5-1 or ENA5-2 at particular concentrations (24). The concentration of the TFO, which caused half of the target duplex to shift to the triplex, corresponded to the dissociation constant K_d of triplex formation (24). Since the intensity of triplex band was smaller than that of duplex band even at 1 μM Pyr15T (see lane 6 for Pyr15T), K_d of the triplex with Pyr15T was estimated to be more than ∼1 μM. In contrast, K_d of the triplex with each of ENA7-1 and ENA7-2 was ∼0.0625 μM, indicating that the ENA modification of TFO at seven positions increased binding constant K_a ($= 1/K_d$) of the pyrimidine motif triplex formation at physiological neutral pH by more than 16-fold. In the meantime, K_d of the triplex with each of ENA5-1 and ENA5-2 was ∼0.125 μM, indicating that the ENA modification of TFO at five positions achieved increase in K_a of the same pyrimidine motif triplex formation by more than 8-fold. The increased number of the ENA modification in TFO enhanced the increased magnitude of K_a for the pyrimidine motif triplex formation at physiological neutral pH.
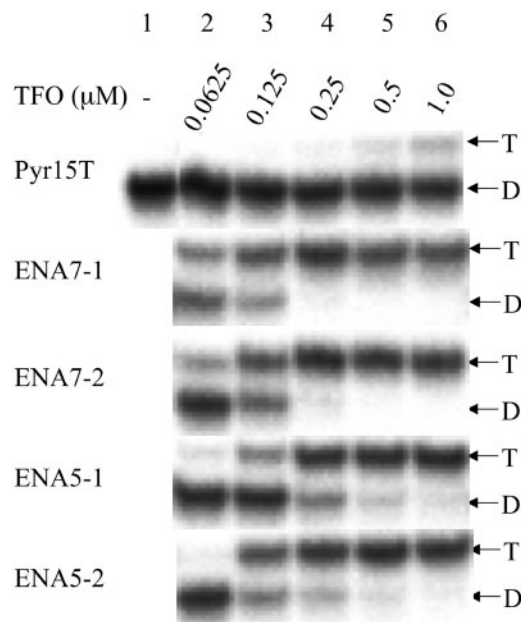

Fig. 2 EMSA of the pyrimidine motif triplex formation using the specific TFOs (Pyr15T, ENA7-1, ENA7-2, ENA5-1 or ENA5-2) at physiological neutral pH. Triplex formation was initiated by adding ³²P-labelled Pur23A•Pyr23T duplex (∼1 nM) with the indicated final concentrations of the specific TFOs (Pyr15T, ENA7-1, ENA7-2, ENA5-1 or ENA5-2). The non-specific oligonucleotide (Pyr15NON) was added to adjust to equimolar concentration (1 μM) of TFO (Pyr15T + Pyr15NON, ENA7-1 + Pyr15NON, ENA7-2 + Pyr15NON, ENA5-1 + Pyr15NON or ENA5-2 + Pyr15NON) in each lane. Reaction mixtures involving Pyr15T, ENA7-1, ENA7-2, ENA5-1 or ENA5-2 in 50 mM tris–acetate (pH 7.0), 100 mM NaCl and 10 mM MgCl₂ were incubated for 6 h at 37°C, and then electrophoretically separated at 4°C on a 15% native polyacrylamide gel prepared in buffer [50 mM tris–acetate (pH 7.0) and 10 mM MgCl₂]. Positions of the duplex (D) and triplex (T) are indicated.

Spectroscopic characterization of pyrimidine motif triplex at physiological neutral pH

We investigated the thermodynamic stability of the pyrimidine motif triplexes involving the unmodified or ENA-modified TFOs at pH 6.8 by UV melting (Fig. 3 and Table I). Two-step melting was observed for the triplexes involving Pyr15T, ENA5-1 or ENA5-2. The first change at the lower temperature T_{m1} corresponded to the melting of the triplex to a duplex and a TFO, and the second change at the higher temperature T_{m2} was the melting of the duplex (Fig. 3). In spite of the almost identical values of T_{m2}, the values of T_{m1} for ENA5-1 or ENA5-2 were remarkably larger than that for Pyr15T by >25°C (Table I). In the meantime, only one transition at higher temperature T_m was observed for the triplexes involving ENA7-1 or ENA7-2. Since UV absorbance change at T_m for ENA7-1 or ENA7-2 was almost equal in magnitude to the sum of those at T_{m1} and T_{m2} for ENA5-1 or ENA5-2 (Fig. 3), we identified that the triplex involving ENA7-1 or ENA7-2 was directly changed into three constituting single-strand DNAs upon the transition at T_m. Thus, the ENA modification of TFO at seven positions achieved the increase in the melting temperature of the triplex by ~50°C (Table I). These results demonstrate that the thermodynamic stability of the triplex involving ENA-modified TFO was remarkably higher than that involving the unmodified TFO, verifying previous result (23) that the ENA modification of TFO thermally stabilized the pyrimidine motif triplex at physiological neutral pH.

To examine the higher order structure of the pyrimidine motif triplexes involving the unmodified or ENA-modified TFOs, we measured CD spectra of triplexes at 20°C and pH 6.8 (Fig. 4). Similar overall form of the CD spectra was observed among all the profiles. A negative band in the short-wavelength (210–220 nm) region typical for the triplex was present in all the profiles, verifying that the triplex was actually formed in all cases of TFO (35). The intensity of the negative short-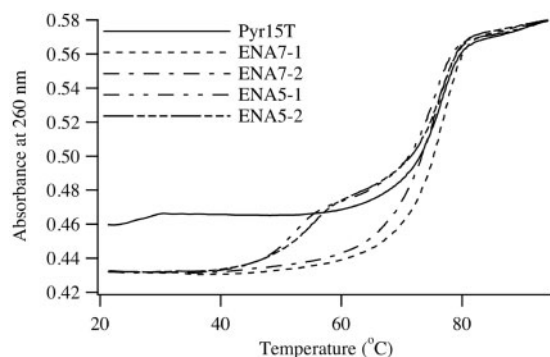wavelength (210–220 nm) band for the triplexes involving the ENA-modified TFOs, ENA7-1, ENA7-2, ENA5-1 or ENA5-2 was larger than that observed for the triplex involving Pyr15T, indicating that all the triplexes involving the ENA-modified TFOs had more features of the A-like conformation than that involving the unmodified TFO (36).

Thermodynamic analyses of pyrimidine motif triplex formation by ITC

We investigated the thermodynamic properties of the pyrimidine motif triplex formation between a 23-bp target duplex (Pur23A•Pyr23T) and its specific 15-mer unmodified (Pyr15T) or ENA-modified (ENA7-1, ENA7-2, ENA5-1 or ENA5-2) TFO at 25°C and pH 6.8 by ITC. To study how the pyrimidine motif triplex formation depends on pH, we also analysed the thermodynamic properties of the triplex formation between Pur23A•Pyr23T and Pyr15T at 25°C and pH 5.8 by ITC. Figure 5A shows a typical ITC curve for the triplex formation between ENA7-1 and Pur23A•Pyr23T at 25°C and pH 6.8. Each injection of Pur23A•Pyr23T into ENA7-1 produced an exothermic heat pulse. The size of each peak was reduced gradually with each new injection, and the last injection still produced a small peak. The area of the small peak was equal to the heat of dilution of Pur23A•Pyr23T obtained from a separate experiment by injecting Pur23A•Pyr23T into the same buffer. We integrated the area under each peak and subtracted the heat of dilution of Pur23A•Pyr23T from the integrated values. We divided the adjusted heat value by the number of moles of injected solution and plotted the obtained values as a function of the molar ratio of [Pur23A•Pyr23T]/[ENA7-1] (Fig. 5B). A sigmoidal plot was fitted to the titration curve by a non-linear least-squares method. The binding constant K_a and the enthalpy change ΔH were calculated from the fitted titration curve (31). The Gibbs free energy change ΔG and the entropy change ΔS were estimated from the equation, $\Delta G = -RT\ln K_a = \Delta H - T\Delta S$, where R is the gas constant and T is the temperature (31). Similarly, we obtained the thermodynamic parameters for pyrimidine motif triplex formation involving each of Pyr15T, ENA7-2, ENA5-1 and ENA5-2 at 25°C and pH 6.8 and for the formation involving Pyr15T at 25°C and pH 5.8. If ENA7-1 is added step-by-step to the Pur23A•Pyr23T solution, it may be necessary to calibrate the heat of dilution of ENA7-1. As described above, when Pur23A•Pyr23T was added step-by-step to the ENA7-1 solution, it was necessary to calibrate

Fig. 3 UV melting profiles of the pyrimidine motif triplexes formed with specific TFOs (Pyr15T, ENA7-1, ENA7-2, ENA5-1 or ENA5-2). The triplexes with Pyr15T, ENA7-1, ENA7-2, ENA5-1 or ENA5-2 in 10 mM sodium cacodylate–cacodylic acid (pH 6.8), 200 mM NaCl and 20 mM MgCl$_2$ were melted at a scan rate of 0.5°C/min with detection at 260 nm. The cell path length was 1 cm. The triplex nucleic acid concentration used was 1 μM.

Table I. Melting temperatures of the triplexes between a 23-bp target duplex (Pur23A•Pyr23T) and a 15-mer TFO (Pyr15T, ENA7-1, ENA7-2, ENA5-1 or ENA5-2) in 10 mM sodium cacodylate–cacodylic acid (pH 6.8), 200 mM NaCl and 20 mM MgCl$_2$.

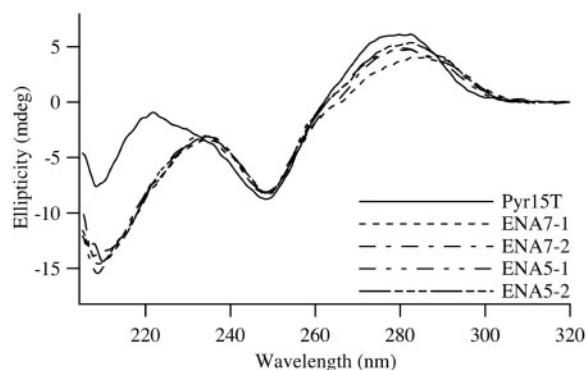| TFO	T_{m1} (°C)	T_{m2} (°C)
Pyr15T	26.8 ± 1.3	76.3 ± 0.3
ENA7-1	76.7 ± 0.2	
ENA7-2	75.5 ± 0.2	
ENA5-1	52.1 ± 0.4	75.7 ± 0.3
ENA5-2	55.2 ± 0.3	76.5 ± 0.3

Fig. 4 CD spectra of the pyrimidine motif triplexes formed with specific TFOs (Pyr15T, ENA7-1, ENA7-2, ENA5-1 or ENA5-2). The triplexes with Pyr15T, ENA7-1, ENA7-2, ENA5-1 or ENA5-2 in 10 mM sodium cacodylate–cacodylic acid (pH 6.8), 200 mM NaCl and 20 mM MgCl$_2$ were measured at 20°C in the wavelength range of 205–320 nm. The cell path length was 1 cm. The triplex nucleic acid concentration used was 1 μM.
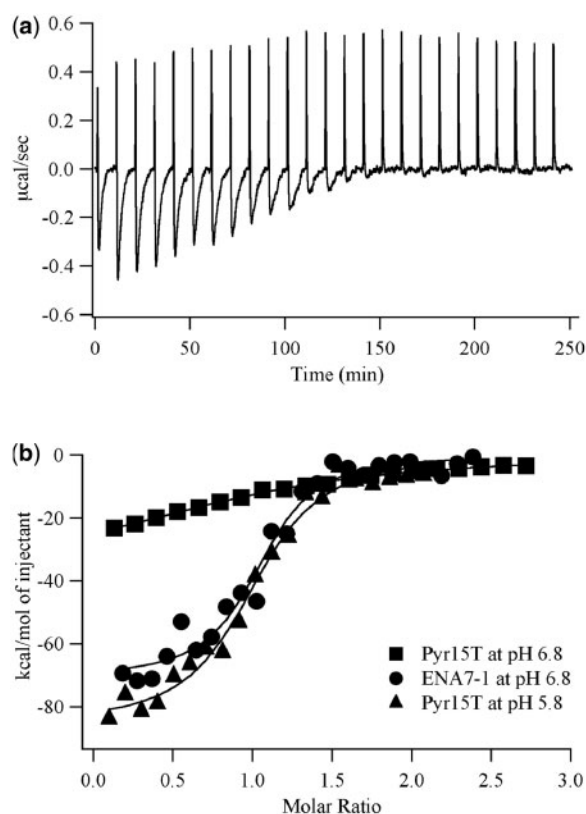

Fig. 5 Thermodynamic analyses of the pyrimidine motif triplex formation at 25°C using Pyr15T or ENA7-1 at pH 6.8 and Pyr15T at pH 5.8 by ITC. (A) Typical ITC profile for the triplex formation between ENA7-1 and Pur23A•Pyr23T at 25°C and pH 6.8. Pur23A•Pyr23T solution (220 μM) in 10 mM sodium cacodylate–cacodylic acid (pH 6.8), 200 mM NaCl and 20 mM MgCl$_2$ was injected 25 times in 5 μl aliquots into ENA7-1 solution (8.5 μM), which was dialyzed against the same buffer. Aliquots were injected over 12 s at 10 min intervals. (B) Titration plots against the molar ratio [Pur23A•Pyr23T]/ [TFO]. The data were fitted by a non-linear least-squares method.

the heat of dilution of Pur23A•Pyr23T. Thus, the situation should be the same in both cases.

Table II summarizes the thermodynamic parameters for the formation of pyrimidine motif triplexes

involving Pyr15T, ENA7-1, ENA7-2, ENA5-1 and ENA5-2 at 25°C and pH 6.8 and for the formation involving Pyr15T at 25°C and pH 5.8, measured by ITC. Negative values of ΔH and ΔS were obtained under each condition. Since a negative ΔS was undesirable for triplex formation, triplex formation was driven by a large absolute value of negative ΔH under each condition. K_a for Pyr15T at pH 5.8 was ~20-fold larger than that obtained for Pyr15T at pH 6.8 (Table II), verifying, like others (6–8), that pyrimidine motif triplex involving C$^+$•G:C triads is unstable at physiological neutral pH. In addition, K_a for ENA7-1 and ENA7-2 at pH 6.8 was ~20-fold larger than that obtained for Pyr15T at pH 6.8 (Table II), indicating that the ENA modification of TFO achieved increase in K_a for pyrimidine motif triplex formation at physiological neutral pH, which was in agreement with the EMSA results (Fig. 2). In the meantime, K_a for ENA5-1 and ENA5-2 at pH 6.8 was ~10-fold larger than that obtained for Pyr15T at pH 6.8 (Table II). The increased magnitude of K_a by ENA modification of TFO at five positions was smaller than that at seven positions. The increased number of the ENA modification in TFO enhanced the increased magnitude of K_a for pyrimidine motif triplex formation at physiological neutral pH, which was in agreement with the EMSA results (Fig. 2). Furthermore, although the K_a and ΔG values for triplex formation involving ENA7-1 and ENA7-2 at pH 6.8 and involving Pyr15T at pH 5.8 were quite similar in magnitude, the ingredients of ΔG, namely, ΔH and ΔS, remarkably differed in value (Table II). The absolute values of the negative ΔH and ΔS for ENA7-1 and ENA7-2 at pH 6.8 were remarkably smaller than those obtained for Pyr15T at pH 5.8 (Table II).

Kinetic analyses of pyrimidine motif triplex formation by BIACORE

To reveal the mechanism for the enhancement of K_a by the ENA modification of TFO (Fig. 2 and Table II), we examined the kinetic parameters for the association and dissociation of TFO (Pyr15T and the ENA-modified TFOs) with Pur23A•Pyr23T at 25°C and pH 6.8 by BIACORE. To study how the pyrimidine motif triplex formation depends on pH, we also analysed the kinetic parameters of the triplex formation between Pur23A•Pyr23T and Pyr15T at 25°C and pH 5.8 by BIACORE. Figure 6A shows typical profiles for the triplex formation and dissociation involving various concentrations of ENA7-1 at 25°C and pH 6.8. Injection of ENA7-1 over the immobilized Bt-Pyr23T•Pur23A increased response. When the concentration of ENA7-1 was increased, response of the association curves was gradually enhanced (Fig. 6A). On-rate constant (k_{on}) for each concentration of ENA7-1 was obtained by analysing each association curve (Fig. 6A). Figure 6B shows a plot of k_{on} against the concentrations of ENA7-1. The plot was fitted to a straight line by a linear least-squares method. The association rate constant (k_{assoc}) was estimated from the slope of the fitted line (33, 34). Off-rate constant (k_{off}) for each concentration of ENA7-1 was obtained by analysing each dissociation curve (Fig. 6A). Since k_{off}

Table II. Thermodynamic parameters for the triplex formation between a 23-bp target duplex (Pur23A•Pyr23T) and a 15-mer TFO (Pyr15T, ENA7-1, ENA7-2, ENA5-1 or ENA5-2) at 25°C, obtained from ITC.

TFO	pH	K_a (M^{-1})	K_a (relative)	ΔG (kcal/mol)	ΔH (kcal/mol)	ΔS (cal/(mol K)
Pyr15T	5.8[a]	$(3.83 \pm 0.74) \times 10^6$	19.4	-8.98 ± 0.13	-85.6 ± 2.6	-257 ± 9
Pyr15T	6.8[b]	$(1.97 \pm 0.43) \times 10^5$	1.0	-7.22 ± 0.15	-34.9 ± 2.2	-93 ± 8
ENA7-1	6.8[b]	$(4.87 \pm 1.62) \times 10^6$	24.7	-9.12 ± 0.24	-63.6 ± 2.6	-183 ± 10
ENA7-2	6.8[b]	$(3.93 \pm 1.60) \times 10^6$	19.9	-9.00 ± 0.31	-63.3 ± 3.5	-182 ± 13
ENA5-1	6.8[b]	$(1.41 \pm 0.35) \times 10^6$	7.2	-8.39 ± 0.17	-64.5 ± 2.5	-188 ± 9
ENA5-2	6.8[b]	$(2.10 \pm 0.62) \times 10^6$	10.7	-8.62 ± 0.21	-66.5 ± 3.5	-194 ± 12

[a]10 mM sodium cacodylate–cacodylic acid (pH 5.8), 200 mM NaCl and 20 mM MgCl$_2$.
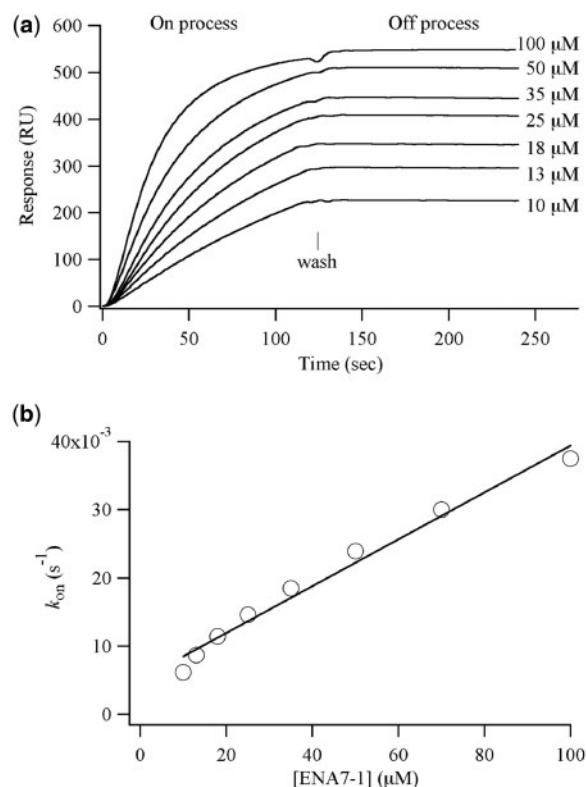[b]10 mM sodium cacodylate–cacodylic acid (pH 6.8), 200 mM NaCl and 20 mM MgCl$_2$.

Fig. 6 Kinetic analyses of the pyrimidine motif triplex formation using ENA7-1 at 25°C and pH 6.8 by BIACORE interaction analysis system. (A) A series of sensorgrams for the triplex formation and the dissociation of the formed triplex between ENA7-1 and Pur23A•Pyr23T at 25°C and pH 6.8. ENA7-1 solutions, diluted in 10 mM sodium cacodylate–cacodylic acid (pH 6.8), 200 mM NaCl and 20 mM MgCl$_2$ to achieve the indicated final concentrations, were injected into the Bt-Pyr23T•Pur23A-immobilized cuvette. The binding of ENA7-1 with Bt-Pyr23T•Pur23A and the dissociation of ENA7-1 from Bt-Pyr23T•Pur23A were monitored as the response against time. (B) Measured on-rate constants k_{on} of the triplex formation in (A) were plotted against the respective concentrations of ENA7-1. The plot was fitted to a straight line ($r^2 = 0.99$) by a linear least-squares method.

is usually independent of the injected TFO concentration, the dissociation rate constant (k_{dissoc}) was estimated from the average of k_{off} for several concentrations of TFO (33, 34). K_a was estimated from the equation, $K_a = k_{assoc}/k_{dissoc}$ (33, 34). Similarly, we obtained the kinetic parameters for pyrimidine motif triplex formation involving each of Pyr15T, ENA7-2, ENA5-1 and ENA5-2 at 25°C and

pH 6.8 and for the formation involving Pyr15T at 25°C and pH 5.8. Although the dissociation phase is not clearly observed in Fig. 6A, it is possible to unambiguously determine k_{off} and k_{dissoc} values from the profile. As shown in k_{dissoc} values of Table III, the magnitudes of the error values are only ∼20% of those of the mean values.

Table III summarizes the kinetic parameters for the formation of pyrimidine motif triplexes involving Pyr15T, ENA7-1, ENA7-2, ENA5-1 and ENA5-2 at 25°C and pH 6.8 and for the formation involving Pyr15T at 25°C and pH 5.8, measured by BIACORE. K_a values estimated from the ratio k_{assoc}/k_{dissoc} (Table III) agreed well with those estimated from ITC (Table II). K_a of the pyrimidine motif triplex formation for Pyr15T at pH 5.8 was ∼60-fold larger than that obtained for Pyr15T at pH 6.8, verifying, like others (6–8), that pyrimidine motif triplex involving C$^+$•G:C triads is unstable at physiological neutral pH. Although the pH shift from 6.8 to 5.8 did not significantly change the k_{assoc}, the k_{dissoc} decreased ∼60-fold by the pH shift, indicating that the much larger K_a at pH 5.8 resulted from the decrease in k_{dissoc}. The ENA modification of TFO at seven positions (ENA7-1 and ENA7-2) increased K_a of the pyrimidine motif triplex formation by ∼70 - to 120-fold, which was in agreement with the results of EMSA (Fig. 2) and ITC (Table II). The k_{dissoc} of the triplex formation decreased ∼190 - to 220-fold by the ENA modification of TFO at seven positions, although ∼1.9- to 2.5-fold smaller k_{assoc} was obtained, which opposes the increase in K_a. In the meantime, the ENA modification of TFO at five positions (ENA5-1 and ENA5-2) increased K_a of the pyrimidine motif triplex formation by ∼30-fold. The k_{dissoc} of the triplex formation decreased ∼60–70-fold by the ENA modification of TFO at five positions, although ∼2.0- to 2.2-fold smaller k_{assoc} was obtained, which opposes the increase in K_a similar to the case of ENA7-1 and ENA7-2. Thus, the decrease in k_{dissoc} resulted in the much larger K_a by the ENA modification of TFO. The increase in K_a by the ENA modification of TFO at seven positions was considerably larger in magnitude than that at five positions. The larger number of the ENA modification in TFO achieved the larger magnitude of the increase in K_a, which was in agreement with the results of EMSA (Fig. 2) and ITC (Table II). The larger magnitude of the increase in K_a by the larger number of the ENA modification resulted from the larger magnitude

Table III. Kinetic parameters for the triplex formation between a 23-bp target duplex (Pur23A•Pyr23T) and a 15-mer TFO (Pyr15T, ENA7-1, ENA7-2, ENA5-1 or ENA5-2) at 25°C, obtained from BIACORE interaction analysis system.

TFO	pH	k_{assoc} (M^{-1} s^{-1})	k_{assoc} (relative)	k_{dissoc} (s^{-1})	k_{dissoc} (relative)	K_a (M^{-1})	K_a (relative)
Pyr15T	5.8[a]	$(5.65 \pm 0.25) \times 10^2$	0.90	$(1.83 \pm 0.49) \times 10^{-4}$	0.016	$(3.09 \pm 1.32) \times 10^6$	57.1
Pyr15T	6.8[b]	$(6.31 \pm 0.18) \times 10^2$	1.0	$(1.17 \pm 0.14) \times 10^{-2}$	1.0	$(5.41 \pm 0.91) \times 10^4$	1.0
ENA7-1	6.8[b]	$(3.43 \pm 0.20) \times 10^2$	0.54	$(5.32 \pm 1.06) \times 10^{-5}$	0.0045	$(6.45 \pm 2.07) \times 10^6$	119
ENA7-2	6.8[b]	$(2.49 \pm 0.11) \times 10^2$	0.40	$(6.36 \pm 1.31) \times 10^{-5}$	0.0054	$(3.92 \pm 1.23) \times 10^6$	72.5
ENA5-1	6.8[b]	$(3.14 \pm 0.11) \times 10^2$	0.50	$(2.08 \pm 0.49) \times 10^{-4}$	0.018	$(1.51 \pm 0.53) \times 10^6$	27.9
ENA5-2	6.8[b]	$(2.81 \pm 0.09) \times 10^2$	0.45	$(1.64 \pm 0.35) \times 10^{-4}$	0.014	$(1.71 \pm 0.53) \times 10^6$	31.6

[a]10 mM sodium cacodylate–cacodylic acid (pH 5.8), 200 mM NaCl and 20 mM $MgCl_2$.
[b]10 mM sodium cacodylate–cacodylic acid (pH 6.8), 200 mM NaCl and 20 mM $MgCl_2$.

of the decrease in k_{dissoc} (~190- to 220-fold decrease for ENA7-1 and ENA7-2 versus ~60—70-fold decrease for ENA5-1 and ENA5-2).

Discussion

K_a of the pyrimidine motif triplex formation involving Pyr15T at pH 5.8 was >20-fold larger than that involving Pyr15T at pH 6.8 (Tables II and III), which agreed well with the previous results that pyrimidine motif triplex involving C^+•G:C triads is unstable at physiological neutral pH (6–8). In addition, K_a of the pyrimidine motif triplex formation involving each of the ENA-modified TFOs at pH 6.8 was >10-fold larger than that involving Pyr15T at pH 6.8 (Tables II and III). The EMSA results (Fig. 2) supported the enhancement of K_a at physiological neutral pH by the ENA modification of TFO. Furthermore, the ENA modification of TFO stabilized the pyrimidine motif triplexes at physiological neutral pH (Fig. 3 and Table I), which verified the previous results (23). Combination of these results shows that the ENA modification of TFO enhances the pyrimidine motif triplex-forming ability at physiological neutral pH.

Since the formed triplex structures involving Pyr15T at pH 5.8 and Pyr15T at pH 6.8 are the same, the absolute values of ΔH and ΔS upon the triplex formation obtained from ITC could in fact be the same for the two conditions. However, ΔH and ΔS for Pyr15T at pH 6.8 were remarkably smaller in magnitude than those obtained for Pyr15T at pH 5.8. When ΔH and ΔS are estimated from the fitting curve of ITC, the value of the heat obtained from ITC is divided not by the effective concentration actually contributed to the triplex formation, but by the superficial concentration added to the triplex formation (31). The estimation does not take into account how many ratio of the added concentration actually contributes to the triplex formation. Therefore, when the triplex formation is substoichiometric under an experimental condition, the absolute values of ΔH and ΔS obtained from ITC should be smaller than those obtained for the more stoichiometric triplex formation under another experimental condition. Thus, the remarkably smaller absolute values of ΔH and ΔS obtained for Pyr15T at pH 6.8 compared with those obtained for Pyr15T at pH 5.8 (Table II) suggest that the triplex formation involving Pyr15T at pH 6.8 was considerably

substoichiometric than that involving Pyr15T at pH 5.8. This was also supported by the remarkably smaller magnitudes of K_a and ΔG for Pyr15T at pH 6.8 (Table II). In contrast, the K_a and ΔG values for Pyr15T at pH 5.8 and those for the ENA-modified TFOs at pH 6.8 were quite similar (Table II), suggesting that the triplex formations under these conditions were similarly quite stoichiometric. We conclude that the triplex formation involving Pyr15T at pH 6.8 was considerably substoichiometric than that involving Pyr15T at pH 5.8 and that involving the ENA-modified TFOs at pH 6.8. Thus, to discuss the mechanism to promote triplex formation by the ENA modification of TFO, the comparison between the absolute values of ΔH and ΔS obtained for Pyr15T at pH 6.8 and those obtained for the ENA-modified TFOs at pH 6.8 is irrelevant owing to the considerably lower stoichiometry for Pyr15T at pH 6.8. The comparison between the absolute values of ΔH and ΔS for Pyr15T at pH 5.8 and those for the ENA-modified TFOs at pH 6.8 with similar stoichiometry will propose a proper mechanism to promote triplex formation by the ENA modification of TFO, as described below.

Although K_a and ΔG for Pyr15T at pH 5.8 and those for the ENA-modified TFOs at pH 6.8 were quite similar in magnitude (Table II), the ingredients of ΔG, namely, ΔH and ΔS, obviously differed in value. The absolute values of the negative ΔH and ΔS obtained for the ENA-modified TFOs at pH 6.8 were smaller than those obtained for Pyr15T at pH 5.8 (Table II). The hydrogen bonding and the base stacking involved in triplex formation mainly contribute to the observed negative ΔH upon triplex formation, obtained from ITC (21, 37–39). The protonation of cytosine bases upon hydrogen bonding and the accompanying deprotonation of the cacodylate buffer dissociating protons to bind with the cytosine bases also contribute to the observed value of ΔH (40). Since the degree of protonation may be similar between the ENA-modified TFOs at pH 6.8 and Pyr15T at pH 5.8 because of the similar stoichiometry described above and as the protons to bind with the cytosine bases are dissociated from the same cacodylate buffer in both cases, the values of ΔH contributed by the protonation of the cytosine bases and the accompanying deprotonation of the cacodylate buffer should be similar in the two cases. Therefore, the different values of ΔH upon formation between the stoichiometric triplexes with

ENA-modified TFOs at pH 6.8 and Pyr15T at pH 5.8 (Table II) suggest that the hydrogen bonding and/or the base stacking of the triplexes involving ENA-modified TFO may remarkably vary from that involving the corresponding unmodified TFO. In fact, the CD spectra show that the triplexes involving ENA-modified TFO had more features of the A-like conformation than that involving the corresponding unmodified TFO (Fig. 4) (*36*). The A-like conformation obtained by the ENA modification of TFO may lead to the different values of the negative ΔH between the unmodified and ENA-modified TFOs. On the other hand, a negative conformational entropy change attributable to the conformational restriction of TFO involved in the triplex formation mainly contributes to the observed negative ΔS upon triplex formation, obtained from ITC (*21, 37–39*). Thus, the smaller absolute value of the negative ΔS for the ENA-modified TFOs at pH 6.8 compared with that for Pyr15T at pH 5.8 (Table II) suggests that the ENA-modified TFO in the unbound state may be more stiff than the corresponding unmodified TFO. The increased stiffness of the modified TFO in the unbound state compared with that of the corresponding unmodified TFO may lead to a smaller loss of conformational entropy upon triplex formation involving the modified TFO at physiological neutral pH, which is favourable to ΔG and increases K_a of triplex formation at physiological neutral pH. We conclude that the increased stiffness of the ENA-modified TFO in the unbound state may be an important factor contributing to promotion of the pyrimidine motif triplex formation at physiological neutral pH.

Kinetic studies revealed that the ENA modification of TFO remarkably decreased k_{dissoc} of the pyrimidine motif triplex formation at physiological neutral pH (Table III). The decrease in k_{dissoc} is a reasonable kinetic factor to describe the considerable increase in K_a at physiological neutral pH by the ENA modification (Fig. 2 and Tables II and III). Both our group (*21*) and others (*41*) formerly suggested a model of triplex formation based on nucleation–elongation processes: in a nucleation stage, only a few Hoogsteen base pairings may be formed between TFO and the target duplex; whereas in an elongation stage, they advance to accomplish triplex formation. Both groups (*21, 41*) also proposed that the obtained K_a, which corresponds to the ratio k_{assoc}/k_{dissoc}, may reflect an equilibrium state of the nucleation stage. The nucleation stage may be the rate-limiting step of the triplex formation. In this context, the ENA modification may slow the breakdown of the nucleation intermediate using the increased stiffness of ENA-modified TFO to promote the pyrimidine motif triplex formation. Due to the increased stiffness of ENA backbone compared with phosphodiester backbone, the ENA-modified TFO may take less number of the possible conformations than the phosphodiester TFO. Therefore, it may take more time for the ENA-modified TFO to search for the conformation, which is able to dissociate from the nucleation intermediate. The longer time to search for the conformation with the ability to dissociate from

the nucleation intermediate may result in smaller k_{dissoc} and larger K_a for the ENA-modified TFO.

The increased magnitude of K_a by the ENA modification at seven positions was larger than that at five positions (Fig. 2 and Tables II and III). In addition, the increased magnitude of thermal stability by the ENA modification at seven positions was also larger than that at five positions (Fig. 3 and Table I). The increased number of the ENA modification in TFO enhanced the increased magnitude of K_a and thermal stability. The more stiffness of TFO by the larger number of the ENA modification may result in the smaller loss of conformational entropy upon triplex formation as discussed above, which is more favourable to ΔG and leads to the larger increase in K_a. This knowledge may be useful to design ENA-modified TFO with higher binding ability in the triplex formation at physiological neutral pH.

The present investigations have obviously indicated that the ENA modification of TFO promoted pyrimidine motif triplex formation at physiological neutral pH. Due to the excellent properties of the ENA modification of TFO, the ENA-modified oligonucleotides may be applicable to various triplex formation-based methods, such as artificial repression of gene expression by antigene strategy, mapping of genomic DNA and gene-targeted mutagenesis. Furthermore, the present investigations have shown that the increased stiffness of the modified TFO in the unbound state may remarkably increase K_a for the pyrimidine motif triplex formation at physiological neutral pH. Our formerly designed chemical modifications of TFO with connection of 2′-*O* and 4′-*C* positions of the sugar group, such as 2′-*O*,4′-*C*-methylene bridged nucleic acid (2′,4′-BNA) (*42, 43*) and 2′-*O*,4′-*C*-aminomethylene bridged nucleic acid (2′,4′-BNA^{NC}) (*44, 45*), also considerably increased K_a for the pyrimidine motif triplex formation at physiological neutral pH. We conclude that the design of TFO, involving the bridging of different positions of the sugar group with an alkyl chain for increased stiffness, is certainly useful to promote the triplex formation at physiological neutral pH and may advance various triplex formation-based methods *in vivo*.

Conflict of interest
None declared.

References
1. Chin, J.Y., Schleifman, E.B., and Glazer, P.M. (2007) Repair and recombination induced by triple helix DNA. *Front Biosci.* **12**, 4288–4297
2. Bissler, J.J. (2007) Triplex DNA and human disease. *Front Biosci.* **12**, 4536–4546

3. Duca, M., Vekhoff, P., Oussedik, K., Halby, L., and Arimondo, P.B. (2008) The triple helix: 50 years later, the outcome. *Nucleic Acids Res.* **36**, 5123–5138

4. Jain, A., Wang, G., and Vasquez, K.M. (2008) DNA triple helices: biological consequences and therapeutic potential. *Biochimie* **90**, 1117–1130

5. Wells, R.D. (2008) DNA triplexes and Friedreich ataxia. *FASEB J.* **22**, 1625–1634

6. Frank-Kamenetskii, M.D. (1992) Protonated DNA structures. *Methods Enzymol.* **211**, 180–191

7. Singleton, S.F. and Dervan, P.B. (1992) Influence of pH on the equilibrium association constants for oligodeoxyribonucleotide-directed triple helix formation at single DNA sites. *Biochemistry* **31**, 10995–11003

8. Shindo, H., Torigoe, H., and Sarai, A. (1993) Thermodynamic and kinetic studies of DNA triplex formation of an oligohomopyrimidine and a matched duplex by filter binding assay. *Biochemistry* **32**, 8963–8969

9. Milligan, J.F., Krawczyk, S.H., Wadwani, S., and Matteucci, M.D. (1993) An anti-parallel triple helix motif with oligodeoxynucleotides containing 2′-deoxyguanosine and 7-deaza-2′-deoxyxanthosine. *Nucleic Acids Res.* **21**, 327–333

10. Cheng, A.J. and Van Dyke, M.W. (1993) Monovalent cation effects on intermolecular purine-purine-pyrimidine triple-helix formation. *Nucleic Acids Res.* **21**, 5630–5635

11. Lee, J.S., Woodsworth, M.L., Latimer, L.J., and Morgan, A.R. (1984) Poly(pyrimidine)·poly(purine) synthetic DNAs containing 5-methylcytosine form stable triplexes at neutral pH. *Nucleic Acids Res.* **12**, 6603–6614

12. Povsic, T.J. and Dervan, P.B. (1989) Triple helix formation by oligonucleotides on DNA extended to the physiological pH range. *J. Am. Chem. Soc.* **111**, 3059–3061

13. Xodo, L.E., Manzini, G., Quadrifoglio, F., van der Marel, G.A., and van Boom, J.H. (1991) Effect of 5-methylcytosine on the stability of triple-stranded DNA: a thermodynamic study. *Nucleic Acids Res.* **19**, 5625–5631

14. Ono, A., Tso, P.O.P., and Kan, L.S. (1991) Triplex formation of oligonucleotides containing 2′-O-methylpseudoisocytidine in substitution for 2′-deoxycytidine. *J. Am. Chem. Soc.* **113**, 4032–4033

15. Krawczyk, S.H., Milligan, J.F., Wadwani, S., Moulds, C., Froehler, B.C., and Matteucci, M.D. (1992) Oligonucleotide-mediated triple helix formation using an N_3-protonated deoxycytidine analog exhibiting pH-independent binding within the physiological range. *Proc. Natl. Acad. Sci. USA* **89**, 3761–3764

16. Koh, J.S. and Dervan, P.B. (1992) Design of a nonnatural deoxyribonucleoside for recognition of Gc base-pairs by oligonucleotide-directed triple helix formation. *J. Am. Chem. Soc.* **114**, 1470–1478

17. Jetter, M.C. and Hobbs, F.W. (1993) 7,8-Dihydro-8-oxoadenine as a replacement for cytosine in the third strand of triple helices. Triplex formation without hypochromicity. *Biochemistry* **32**, 3249–3254

18. Ueno, Y., Mikawa, M., and Matsuda, A. (1998) Nucleosides and nucleotides. 170. Synthesis and properties of oligodeoxynucleotides containing 5-[N-[2-[N,N-bis(2-aminoethyl)- amino]ethyl]carbamoyl]-2′-deoxyuridine and 5-[N-[3-[N,N-bis(3-aminopropyl) amino]propyl]carbamoyl]-2′-deoxyuridine. *Bioconjug. Chem.* **9**, 33–39

19. Sun, J.S., Giovannangeli, C., Francois, J.C., Kurfurst, R., Montenay-Garestier, T., Asseline, U., Saison-Behmoaras, T., Thuong, N.T., and Helene, C. (1991) Triple-helix formation by alpha oligodeoxynucleotides and alpha oligodeoxynucleotide-intercalator conjugates. *Proc. Natl. Acad. Sci. U A* **88**, 6023–6027

20. Mouscadet, J.F., Ketterle, C., Goulaouic, H., Carteau, S., Subra, F., Le Bret, M., and Auclair, C. (1994) Triple helix formation with short oligonucleotide-intercalator conjugates matching the HIV-1 U3 LTR end sequence. *Biochemistry* **33**, 4187–4196

21. Kamiya, M., Torigoe, H., Shindo, H., and Sarai, A. (1996) Temperature dependence and sequence specificity of DNA triplex formation: an analysis using isothermal titration calorimetry. *J. Am. Chem. Soc.* **118**, 4532–4538

22. Morita, K., Hasegawa, C., Kaneko, M., Tsutsumi, S., Sone, J., Ishikawa, T., Imanishi, T., and Koizumi, M. (2002) 2′-O,4′-C-ethylene-bridged nucleic acids (ENA): highly nuclease-resistant and thermodynamically stable oligonucleotides for antisense drug. *Bioorg. Med. Chem. Lett.* **12**, 73–76

23. Koizumi, M., Morita, K., Daigo, M., Tsutsumi, S., Abe, K., Obika, S., and Imanishi, T. (2003) Triplex formation with 2′-O,4′-C-ethylene-bridged nucleic acids (ENA) having C3′-endo conformation at physiological pH. *Nucleic Acids Res.* **31**, 3267–3273

24. Lyamichev, V.I., Mirkin, S.M., Frank-Kamenetskii, M.D., and Cantor, C.R. (1988) A stable complex between homopyrimidine oligomers and the homologous regions of duplex DNAs. *Nucleic Acids Res.* **16**, 2165–2178

25. Torigoe, H., Ferdous, A., Watanabe, H., Akaike, T., and Maruyama, A. (1999) Poly(L-lysine)-graft-dextran copolymer promotes pyrimidine motif triplex DNA formation at physiological pH: thermodynamic and kinetic studies. *J. Biol. Chem.* **274**, 6161–6167

26. Torigoe, H. (2001) Thermodynamic and kinetic effects of $N_3′$→$P5′$ phosphoramidate modification on pyrimidine motif triplex DNA formation. *Biochemistry* **40**, 1063–1069

27. Torigoe, H. and Maruyama, A. (2005) Synergistic stabilization of nucleic acid assembly by oligo-N3′→P5′ phosphoramidate modification and additions of comb-type cationic copolymers. *J. Am. Chem. Soc.* **127**, 1705–1710

28. Torigoe, H., Sasaki, K., and Katayama, T. (2009) Thermodynamic and kinetic effects of morpholino modification on pyrimidine motif triplex nucleic acid formation under physiological condition. *J. Biochem.* **146**, 173–183

29. Langerman, N. and Biltonen, R.L. (1979) Microcalorimeters for biological chemistry: applications, instrumentation and experimental design. *Methods Enzymol.* **61**, 261–286

30. Biltonen, R.L. and Langerman, N. (1979) Microcalorimetry for biological chemistry: experimental design, data analysis, and interpretation. *Methods Enzymol.* **61**, 287–318

31. Wiseman, T., Williston, S., Brandts, J.F., and Lin, L.N. (1989) Rapid measurement of binding constants and heats of binding using a new titration calorimeter. *Anal. Biochem.* **179**, 131–137

32. Torigoe, H., Shimizume, R., Sarai, A., and Shindo, H. (1999) Triplex formation of chemically modified homopyrimidine oligonucleotides: thermodynamic and kinetic studies. *Biochemistry* **38**, 14653–14659

33. Edwards, P.R., Gill, A., Pollard-Knight, D.V., Hoare, M., Buckle, P.E., Lowe, P.A., and Leatherbarrow, R.J. (1995) Kinetics of protein–protein interactions at the surface of an optical biosensor. *Anal. Biochem.* **231**, 210–217

34. Bates, P.J., Dosanjh, H.S., Kumar, S., Jenkins, T.C., Laughton, C.A., and Neidle, S. (1995) Detection and kinetic studies of triplex formation by oligodeoxynucleotides using real-time biomolecular interaction analysis (BIA). *Nucleic Acids Res.* **23**, 3627–3632

35. Manzini, G., Xodo, L.E., Gasparotto, D., Quadrifoglio, F., van der Marel, G.A., and van Boom, J.H. (1990) Triple helix formation by oligopurine-oligopyrimidine DNA fragments: electrophoretic and thermodynamic behavior. *J. Mol. Biol.* **213**, 833–843

36. Johnson, K.H., Gray, D.M., and Sutherland, J.C. (1991) Vacuum UV CD spectra of homopolymer duplexes and triplexes containing A.T or A.U base pairs. *Nucleic Acids Res.* **19**, 2275–2280

37. Edelhoch, H. and Osborne, J.C. Jr (1976) The thermodynamic basis of the stability of proteins, nucleic acids, and membranes. *Adv. Protein Chem.* **30**, 183–250

38. Cheng, Y.K. and Pettitt, B.M. (1992) Stabilities of double- and triple-strand helical nucleic acids. *Prog. Biophys. Mol. Biol.* **58**, 225–257

39. Shafer, R.H. (1998) Stability and structure of model DNA triplexes and quadruplexes and their interactions with small ligands. *Prog. Nucleic Acid Res. Mol. Biol.* **59**, 55–94

40. Fukada, H. and Takahashi, K. (1998) Enthalpy and heat capacity changes for the proton dissociation of various buffer components in 0.1 M potassium chloride. *Proteins* **33**, 159–166

41. Rougee, M., Faucon, B., Mergny, J.L., Barcelo, F., Giovannangeli, C., Garestier, T., and Helene, C. (1992) Kinetics and thermodynamics of triple-helix formation: effects of ionic strength and mismatches. *Biochemistry* **31**, 9269–9278

42. Torigoe, H., Hari, Y., Sekiguchi, M., Obika, S., and Imanishi, T. (2001) 2′-*O*,4′-*C*-methylene bridged nucleic acid modification promotes pyrimidine motif triplex DNA formation at physiological pH: thermodynamic and kinetic studies. *J. Biol. Chem.* **276**, 2354–2360

43. Torigoe, H., Maruyama, A., Obika, S., Imanishi, T., and Katayama, T. (2009) Synergistic stabilization of nucleic acid assembly by 2′-*O*,4′-*C*-methylene-bridged nucleic acid modification and additions of comb-type cationic copolymers. *Biochemistry* **48**, 3545–3553

44. Torigoe, H., Rahman, S.M., Takuma, H., Sato, N., Imanishi, T., Obika, S., and Sasaki, K. (2011) 2′-*O*,4′-*C*-aminomethylene-bridged nucleic acid modification with enhancement of nuclease resistance promotes pyrimidine motif triplex nucleic acid formation at physiological pH. *Chemistry* **17**, 2742–2751

45. Torigoe, H., Rahman, S.M., Takuma, H., Sato, N., Imanishi, T., Obika, S., and Sasaki, K. (2011) Interrupted 2′-*O*,4′-*C*-aminomethylene bridged nucleic acid modification enhances pyrimidine motif triplex-forming ability and nuclease resistance under physiological condition. *Nucleosides Nucleotides Nucleic Acids* **30**, 63–81